NASA Jet Propulsion Laboratory, Caltech SURF Report

Atmospheric Correction Using Deep Neural Networks

Shubhankar V. Deshpande

Mentor : David R. Thompson

1 Abstract

An open problem in imaging spectroscopy is generating an accurate model of the atmosphere. Physical properties of the atmosphere cannot be directly modeled, and hence this becomes an inverse problem, where a proxy quantity is measured, to derive atmospheric properties. The optical effects are captured within the radiative transfer equation (RTE), solving of which entails constraining the boundary conditions captured as an initial state vector. Optimal Estimation is a method used for the inverse problem of retrieving an accurate state vector. However, the major hurdle is the computational cost associated with running the forward model numerous times. Under certain assumptions, using the universal approximation theorem, we may approximate this continuous function using a multilayer perceptron. We simulate data to generate a high-dimensional parameter space, which is run through the forward model (RTE) to synthesize radiance values, which are decomposed to generate a simpler model. Our model reproduces the mapping to within numerical precision after being trained using state of the art deep learning techniques resulting in a multi-fold speedup. Further, we designed an automated system to track the data product flow at process level granularity. The consolidated system results in a streamlined pipeline, reducing the time to generate scientific results.

2 Overview

2.1 Imaging Spectroscopy

The concept of imaging spectroscopy entails measuring a grid of radiances in multiple contiguous spectral channels. These images are acquired through the use of an imaging spectrometer supported onboard an airborne or orbital platform.

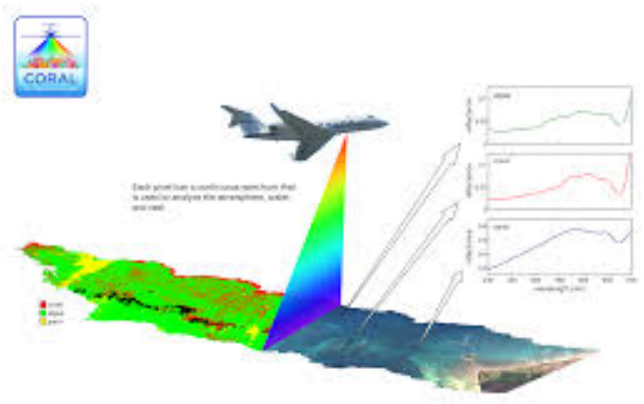

Figure 1: Imaging Spectrometer NASA-JPL/BIOS

2.2 Radiative Transfer

The radiative transfer equation (RTE), models atmospheric interactions such as the energy lost through absorption, gained by emission, and subsequent redistribution through scattering.

$$\frac{1}{c}\frac{\partial}{\partial t}I_\nu + \hat{\Omega}\cdot\nabla I_\nu + (k_{\nu,s}+k_{\nu,a})I_\nu = j_\nu + \frac{1}{4\pi}k_{\nu,s}\int_\Omega I_\nu d\Omega \quad (1)$$

Where

$$j_\nu \rightarrow EmissionCoefficient$$

$$k_{\nu,s} \rightarrow ScatteringOpacity$$

$$k_{\nu,a} \rightarrow AbsorptionOpacity$$

A complete explanation of the radiative transfer equation is beyond the scope of this paper however, the reader is encouraged to refer to [3] for an in-depth analysis and discussion regarding radiative transfer modeling. Analytic solutions to the RTE exist for simplified assumptions, but for complex modeling, numerical methods are required. Traditional numerical methods such as Monte Carlo, are encapsulated as solvers in radiative transfer codes such as libRadtran.

2.3 Atmospheric Correction

The quantity measured by an imaging spectrometer, which is typically solar radiance, is subject to atmospheric effects such as absorption and scattering. Thus, in order to accurately study surface properties, these atmospheric effects must be taken into account and corrected for, in a process called atmospheric correction. The process in which this is done has evolved over time from empirical line based methods to more recent approaches such as modeling using the radiative transfer equation. Succinctly, the typical atmospheric correction process is structured as

1. An initial guess for the state vector (contains representative properties of atmospheric conditions)

2. Using the parameters of the initial state vector to constrain the boundary conditions of the radiative transfer equation

3. Solving (through numerical methods) to obtain a unique set of radiance values per band (depending on the spectral resolution)

4. Reverse propagating the values through Optimal Estimation, to obtain a better estimate of the original state vector

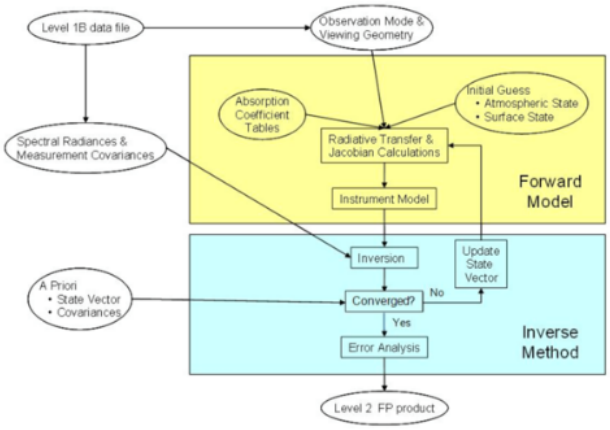

Figure 2: Process of Atmospheric Correction [1]

This is repeated millions of times during the typical lifetime of the process. A significant drawback to obtaining an accurate estimate of the state vector, is the sheer computational requirement associated with solving the complex radiative transfer model multiple times using numerical methods. Hence, it is imperative to design faster methods that will enable better science results downstream.

2.4 Neural Networks

Neural Networks are non-linear function estimators that are used for a variety of tasks from regression to classification. They are particularly useful in a high dimensional parameter space where they are able to efficiently fit accurate hyperplanes.

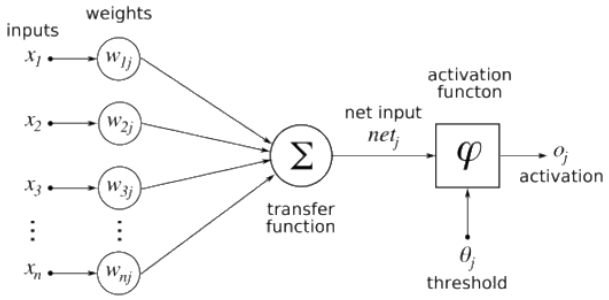

Figure 3: Neuron [2]

The basic unit of a neural network is a neuron, which consists of a transfer function and an activation function. The transfer function multiplies the inputs by a set of weights, which is then passed through an activation function. The activation function is a nonlinearity such as the hyperbolic tan, the rectified linearity, sigmoid, etc. A number of such neurons are then cascaded together to form a large hierarchical model which is able to learn complicated distributions of data.

2.5 Universal Approximation Theorem

The Universal Approximation Theorem states that a feed-forward network with at least one hidden layer containing a finite number of neurons (i.e. a multilayer perceptron), can approximate continuous functions on a compact subset of $\mathbb{R}^n$, under certain assumptions of the activation function.
More precisely,
Let $\varphi(\cdot)$ be a nonconstant, bounded, and monotonically increasing continuous function. Let I_m denote the m-dimensional unit hypercube $[0,1]^m$. The space of continuous functions on I_m is denoted by $C(I_m)$. Then given any $\varepsilon > 0$ and any function $f \in C(I_m)$, there exists an integer N, real constants $v_i, b_i \in \mathbb{R}$ and real vectors $w_i \in \mathbb{R}^m$ where $i = 1, \cdots, N$ such that we can define:

$$F(x) = \sum_{i=1}^{N} v_i \varphi(w_i^T x + b_i) \tag{2}$$

such that $\forall x \in I_m$

$$|F(x) - f(x)| < \epsilon \tag{3}$$

3 Method

3.1 Dataset Synthesis

An optimal set of parameters was chosen would enable the model to generalize well for real-life scenarios. This included:

1. Wavelength $(\lambda) \in [740, 800]$ Nanometer
2. Albedos $\in [0, 100]$ %
3. Visibility Conditions $\in [6, 100]$ Kilometers
4. Default Aerosol Conditions (libRadtran)

The radiance quantity which is measured by the imaging spectrometer can be analytically decomposed to reflectance.

$$\rho = \frac{\pi L}{\cos\theta} \tag{4}$$

Where

$$L \rightarrow RadianceatSensor$$

$$F \rightarrow SolarIrradiance$$

$$\theta \rightarrow SolarZenithAngle$$

A choice was made to model this intermediate quantity instead of the radiance directly due to the following reasons

- More stable output target, resulting in a reduction in variation.
- Decouples the radiative transfer modeling from the solar input function.

The TOA reflectance can further be decomposed into intermediate quantities such as transmission, albedo, and surface reflectance through the synthesis of TOA at three constant albedos and using basic algebraic manipulation.

$$\rho_{TOA} = \rho_{ATM} + \frac{T\rho_s}{1 - S\rho_s} \tag{5}$$

Where

$$T \rightarrow Transmission$$

$$S \rightarrow SphericalAlbedo$$

$$\rho_s \rightarrow SurfaceReflectance$$

Fitting the model on these simpler quantities results in a higher final accuracy, recombination of which yields the TOA reflectance.

3.2 Network Architecture

A custom architecture was designed to capture the underlying physical parameter space. The complete network consists of

- **Auxiliary Support Nodes**:
  Responsible for supplying a normalized input space to the constituent subnetworks.
- **Monochromatic Subnetworks**:
  Responsible for predicting the value for a single band.

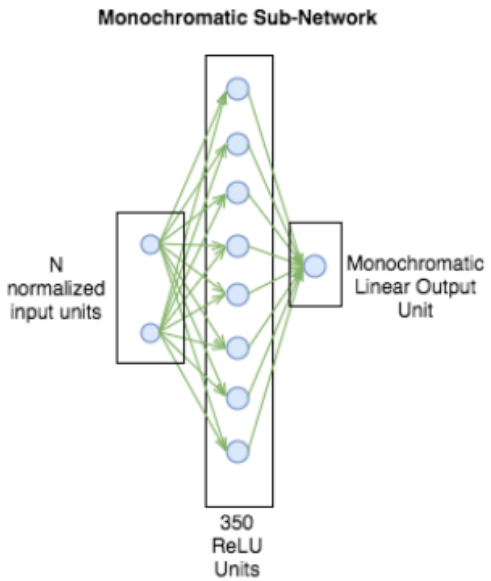

Figure 4: Monochromatic Subnetwork

A collection of N such monochromatic subnetworks predicting the value per band results in the entire spectrum.

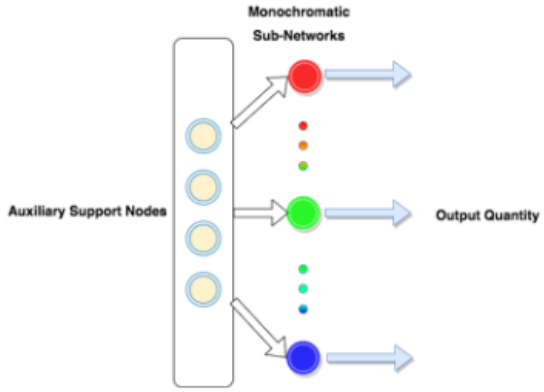

Figure 5: ACDNN

3.3 Results

The custom designed network architecture was implemented using a mixture of Keras [4] and Tensorflow [5], and trained on a high-performance supercomputer cluster optimized for parallel computation using state of the art deep learning techniques proved to perform well on a variety of machine learning tasks. The error metric used for evaluation was least mean squares, which resulted in an average error of $7 * 10^{-6}$, using 10-fold cross-validation.

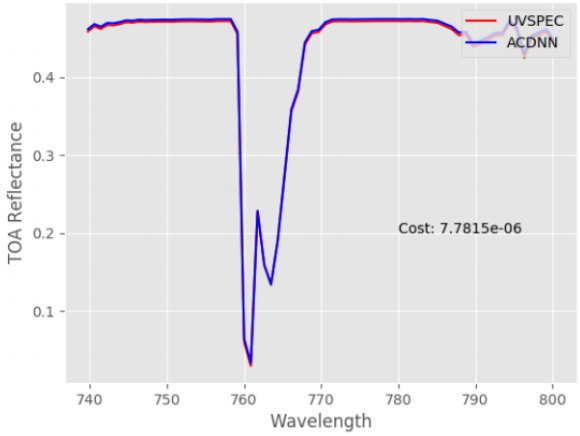

Figure 6: Plot of Predicted Output

3.4 Future Work

Future directions include expanding the physical parameter space to synthesize a spectrum influenced by a larger state vector. Once this larger parameter space has been incorporated to generate a model of higher complexity, we will then proceed to test the model across a constrained space of sample data.

4 Automated Storage & Integration System

4.1 Data Consolidation & Archival Tracking

Sensitivity measurements are bound to evolving configuration formats, due to upgradation in hardware capabilities as the lifecycle of the project progresses. This creates a hindrance in the time to generate data driven scientific results, as a significant amount of time must be invested by the researcher to process these files of varying configuration formats. A next-generation system must be created that can efficiently process data across various configuration formats as needed, depending on the specific case. The system should further be able to track the current state of the archive on the basis of defined characteristics, across all components of the pipeline. This consolidated system would result in a more streamlined data workflow, which would potentially reduce the time to generate data-driven scientific results.

4.2 Objectives

The prime objective of the system is to create a next-generation science data workflow by streamlining the existing pipeline. The system improves the efficiency of analysis, through the reduction in manual workload. The system could further be used to improve the automation of the analysis through a global configuration database. The workflow has been automated to track the current state of the archive by abstracting the processing flow to the granularity of degree of processing. The tracking is characterized by features such as:

1. Which files have been analyzed, and level to which every file been processed in the pipeline
2. Where are the files stored in the system
3. Associated metadata (date of creation, date changed)

Concretely the baseline level of efficiency for this system is characterized through a higher degree of data insight coupled with a reduced system complexity, ease of integration with current SDS, and an improvement in the data product generation latency.

5 Method

The specifications of the current versions of the L1B products and L2B products may be found at [15] and [16]. Prior to initiating work on the project, a hands-on systems orientation was given, to gain domain level insight to the data flowing through the system.

[1] NASA Jet Propulsion Laboratory, California Institute of Technology

Upon project initiation, a multi-step procedure of satisfying the objectives occurred in the following manner:

1. A hands-on orientation to the SDS, where a detailed interaction was done with the SDS team to understand in further depth the nature of the system.
2. A requirements elicitation phase to ensure efficient and precise gathering of the features to be introduced.
3. The design of the archival state tracking mechanism to cover all required characteristics.
4. Installation and configuration of pre-requisite software packages, along with the transfer of configuration data into a NoSQL (MongoDB) data store to account for the heterogenous nature of the data.
5. A prototype implementation of the parser + state tracking mechanism across a small section of the pipeline.
6. An iterative approach to development to converge on target performance measures through the generation of statistics to log current system performance.
7. Running an A/B test to ensure that the system integrates well into the current SDS, and to mitigate any possible challenges.

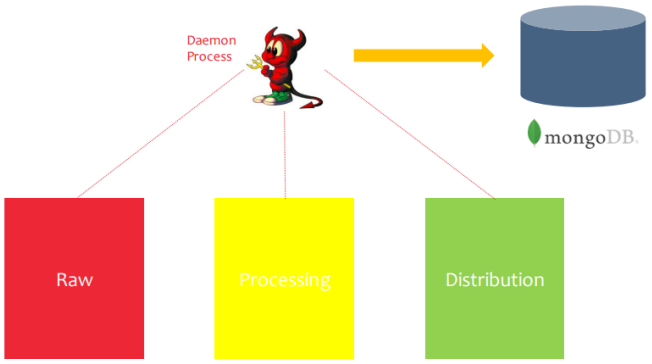

Figure 7: ASIST System

Acknowledgements

I thank Dr.David R. Thompson[1] for offering me the opportunity to contribute to the CORAL project. His continued support & guidance on conducting research has been a constant source of inspiration. I would further like to thank Winston Olson-Duvall[1] and Sarah Lundeen[1] for providing valuable insights into the working of the SDS and explaining the intracacies of the system.

References

[1] David Crisp, Hartmut Boesch, et al. *Orbiting Carbon Observatory (OCO)-2 Level 2 Full Physics Algorithm Theoretical Basis Document Version 2.0 Rev 0*. May 17, 2014

[2] Artificial neural network. *Artificial neural network - Wikimedia Commons*, commons.wikimedia.org/wiki/Artificial_neural_network. Accessed 26 Sept. 2017.

[3] Chandrasekhar, S. *Radiative transfer.* Oxford, University Press, 1950.

[4] Chollet, François et al. *Keras* GitHub, 2015, https://github.com/fchollet/keras

[5] Abadi, Martin et al.*TensorFlow: Large-Scale Machine Learning on Heterogeneous Systems*, 2015. Software available from tensorflow.org

[6] Goodfellow, Ian, et al. *Deep learning*. Cambridge, MA, The MIT Press, 2017.

[7] I. E. Lagaris, A. Likas and D. I. Fotiadis, 1997 *Artificial Neural Networks for Solving Ordinary and Partial Differential Equations*

[8] Artificial neural network. *Wikipedia*, Wikimedia Foundation, 23 Sept. 2017, en.wikipedia.org/wiki/Artificial_neural_network. Accessed 26 Sept. 2017.

[9] Universal approximation theorem. *Wikipedia*, Wikimedia Foundation, 17 Sept. 2017, en.wikipedia.org/wiki/Universal_approximation_theorem. Accessed 26 Sept. 2017.

[10] Buras et al *J. Quant. Spectr. Ra. Tran. 112, 2028-2034, doi:10.1016/j.jqsrt.2011.03.019*

[11] *International Society for Reef Studies Consensus Statement, October 2015*

[12] *Biogeophysical Components of Influence on Reefs*, https://coral.jpl.nasa.gov/about-coral

[13] *Data Processing Levels for EOSDIS Data Products*, https://science.nasa.gov/earth-science/earth-science-data/data-processing-levels-for-eosdis-data-products

[14] *Data Products Specification for CORAL*, https://coral.jpl.nasa.gov/data-products

[15] *CORAL L1 Distribution Document v03*, https://coral.jpl.nasa.gov/alt_locator/CORAL_L1B_Data_Product_Readme_v04.txt

[16] *CORAL L2 Distribution Document v02*, Available at https://coral.jpl.nasa.gov/alt_locator/CORAL_L2_Data_Product_Readme_v02.txt

Appendix

About CORAL

According to a recent investigation, an estimated 33-50 % of the world's coral reefs have undergone degradation, believed to be as a result of climate change [11]. However, the data supporting the investigation are scattered, and the exact relation it has to the environmental condition cannot be easily established. In order to better predict the future of the global reef ecosystem, the CORAL campaign will explore the relation between the environmental condition and influential biogeophysical parameters. The objectives of the CORAL campaign as stated [12] are:

- To measure the condition of representative coral reefs across the global range of reef biogeophysical values. The primary indicators for coral reef condition are benthic cover (ratio of coral, algae, and sand), primary productivity, and calcification.

- To establish empirical models that relate reef condition to biogeophysical forcing parameters. Ten primary biogeophysical parameters have been selected for their recognized influence on components of the reef system. [12]

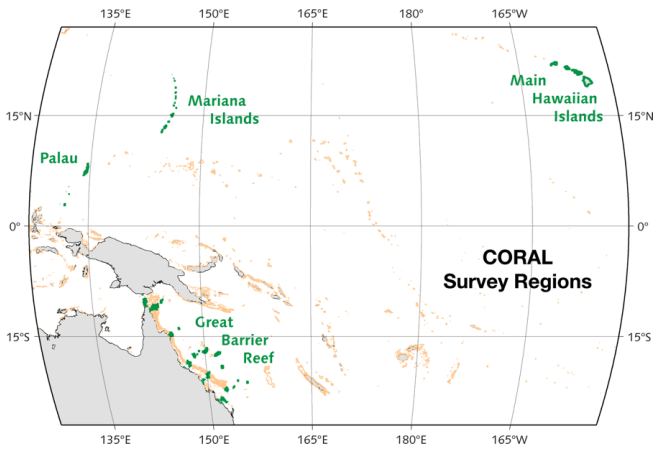

Figure 8: CORAL Survey Area [12]

The CORAL project consists of a hierarchical multilayer data processing system, the Software Data System (SDS), that processes data products at various levels in accordance with the specification for EOSDIS data products. [13]

[2]http://coral.jpl.nasa.gov.

Data Product	Description
Level 0	Reconstructed, unprocessed PRISM digitized numbers (DN) at full resolution with GPS
Level 1	Calibrated spectral radiance with geolocation information including illumination and observation geometry
Level 2	Benthic reflectance generated following atmosphere and water column radiative transfer inversion with geolocation, support processing information and flags
Level 3	Benthic cover, i.e., seafloor classified into coverage of benthic types (coral, algae, sand) with geolocation, uncertainties, and flags
Level 4	Benthic primary productivity and calcification

Table 1: Data Products [14]

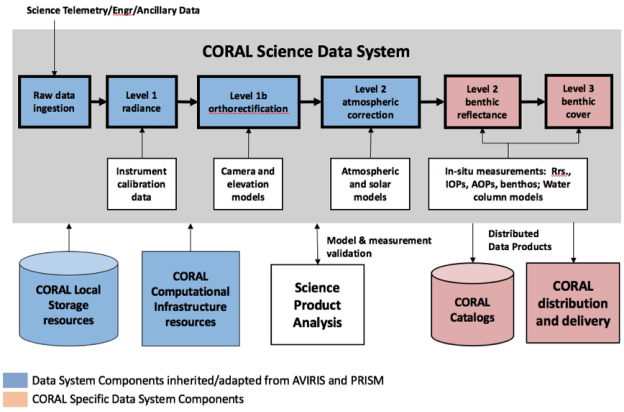

Figure 9: CORAL Data System [14]

More information regarding the CORAL project and the PRISM imaging spectrometer may be found on the project website. [2]